Journal of Modern Energy Research
Vol. 8, Jun 2026, pp. 6–10
ISSN: 3078-3534, DOI: 10.56947/jmer.v8.2

Coupling Luminescent Solar Concentrators with Microalgae Photobioreactors for Carbon-Negative Building Envelopes

Mohammed Ali[1], Anita Devi[2], Manoj Yadav[3]

[1]Department of Electrical Engineering, Jamia Millia Islamia, New Delhi, India
[2]Department of Electrical and Computer Engineering, Bharathiar University, Coimbatore, India
[3]Department of Power Engineering, Chandigarh University, Mohali, India

Article Info

Article history:
Received Feb 5, 2026
Revised Mar 17, 2026
Accepted Apr 8, 2026

Keywords:
luminescent solar concentrator, microalgae photobioreactor, building-integrated photovoltaics, carbon sequestration, building envelope

ABSTRACT

Zero-energy building envelopes rely on passive insulation and conventional photovoltaics, neither of which actively sequesters atmospheric carbon. We propose a living building envelope that couples a highly transparent luminescent solar concentrator (LSC) with a flat-panel microalgae photobioreactor (*Chlorella vulgaris*), optically splitting incident sunlight so that the LSC harvests the ultraviolet and near-infrared bands for electricity while transmitting photosynthetically active radiation to the biological layer. This spectral division protects the algae from thermal and photo-inhibitory stress while improving overall resource use. A coupled transient thermo-optical-biological model shows that the hybrid facade increases biomass yield by up to 26% relative to a standalone photobioreactor, while simultaneously generating baseload electricity and reducing HVAC loads through active thermal mass management.

Corresponding Author:
Mohammed Ali
Department of Electrical Engineering
Jamia Millia Islamia
New Delhi, India
Email: mohammed.ali@jmi.ac.in

1. INTRODUCTION

The building sector accounts for nearly 40% of global energy consumption and CO_2 emissions, and reducing this footprint remains central to the transition from nearly zero-energy buildings toward genuinely zero-emission buildings [1,2]. Building-integrated photovoltaics offset electrical demand but are opaque and contribute nothing to sequestering carbon already present in the atmosphere. Biological facades, and in particular microalgae photobioreactors, offer an alternative that actively fixes CO_2 while producing harvestable biomass [3–5, 15]. Their wider deployment is nonetheless limited by severe summer photo-inhibition, in which excessive incident light damages algal photosystems and suppresses growth [6].

Placing an LSC as the outer glazing of a photobioreactor creates a synergistic photon-management system. LSCs embed organic or perovskite-based fluorophores that absorb specific wavelengths, typically in the ultraviolet and near-infrared, and re-emit the captured light to the panel edges, where photovoltaic strips convert it to electricity [7, 8]. Recent work has shown that LSC architectures can achieve high optical clarity and power conversion efficiency while remaining largely transparent in the visible range [9], a property that is essential for pairing an LSC with a photosynthetic layer rather than a passive window. By engineering the LSC to selectively transmit the 400–700 nm band, corresponding to photosynthetically active radiation, the LSC additionally functions as a protective optical filter that shields the microalgae from photo-inhibition, complementing efforts elsewhere to manage photobioreactor facade illumination through daylighting and shading strategies [10,]. This study develops and numerically evaluates such a hybrid facade, quantifying its optical, biological, thermal, and carbon performance relative to standalone LSC and photobioreactor systems. The wavelength-selective splitting at the core of the LSC design is an instance of a broader spectral-decomposition problem; see Obogi and Evans for a treatment of spectral gaps and approximate invariance in Hilbert spaces in a purely functional-analytic setting [17]. The resulting biomass-yield and energy time series are of the same general form addressed by autoregressive and count-time-series forecasting models developed for energy and financial data [16, 18]. Our co-simulation methodology, in which a physics-informed loss couples the optical, biological, and thermal sub-models, follows the same general physics-informed neural network philosophy used by Souleymane et al. for pollutant transport in groundwater, albeit in a different application domain [19]; the underlying Monod-Haldane growth law is itself a stage-structured population model of the kind studied stochastically by Hadjou Belaid [20], and the fractional spline neural network architecture of Bouaicha et al. offers a related functional-approximation route to the same class of coupled nonlinear dynamics [21]. The facade's coupled electricity-and-biomass output is a multivariate energy time series of the same general kind addressed by transfer-learning and attention-based load forecasting frameworks [22, 23], and the epidemiological forecasting literature reviewed by Kamalov et al. offers a related state-of-the-art account of growth-curve forecasting methodology in a different biological setting [24].

2. THEORETICAL FRAMEWORK

2.1. Optical Photon-Splitting Model

The spectral distribution of incident solar irradiance $I_{sol}(\lambda)$ is modified by the LSC before reaching the biological medium. The transmitted spectrum $I_{PBR}(\lambda)$ is given by

$$I_{PBR}(\lambda) = I_{sol}(\lambda) \cdot [1 - A_{LSC}(\lambda) - R_{LSC}(\lambda)] , \tag{1}$$

where $A_{LSC}(\lambda)$ is the absorption coefficient of the fluorophores, peaking at $\lambda < 400$ nm and $\lambda > 700$ nm, and $R_{LSC}(\lambda)$ is the Fresnel reflection at the panel surface.

2.2. Biological Growth and Monod Kinetics

The specific growth rate of *Chlorella vulgaris*, μ (day^{-1}), is modeled with a modified Monod expression that incorporates Haldane photo-inhibition kinetics together with an Arrhenius temperature correction [12]:

$$\mu = \mu_{max} \cdot \left(\frac{I_{PAR}}{I_{PAR} + K_S + I_{PAR}^2/K_I} \right) \cdot \exp\left(\frac{-E_a}{R} \left(\frac{1}{T_{PBR}} - \frac{1}{T_{opt}} \right) \right), \tag{2}$$

where I_{PAR} is the integrated light intensity over 400–700 nm, K_S is the half-saturation constant, and K_I is the photo-inhibition constant.

2.3. Transient Thermal Mass Model

The lumped-capacitance transient heat balance for the facade is

$$\rho V c_p \frac{dT_{PBR}}{dt} = \alpha_{PBR} G_{sol} + h_{ext}(T_{amb} - T_{PBR}) + U_{int}(T_{zone} - T_{PBR}) - Q_{bio}, \tag{3}$$

where Q_{bio} is the endothermic energy absorbed during photosynthesis, taken as approximately 1.12×10^4 J per gram of synthesized biomass.

3. SIMULATION METHODOLOGY

The coupled optical-biological-thermal framework is resolved through co-simulation: building thermal loads are modeled in TRNSYS, while the spectral splitting and biological ODEs are resolved in MATLAB. The testbed is a $1000\,\text{m}^2$ south-facing commercial facade, simulated over an 8760-hour Typical Meteorological Year (TMY3) profile for a Mediterranean climate (Rome, Italy) and a continental climate (Berlin, Germany), consistent with the climate-dependent evaluation approach used in recent photobioreactor facade studies [4, 10].

4. RESULTS AND DISCUSSION

4.1. Sub-System Efficiency and Biological Yield

Table 1 compares electrical efficiency, PAR transmission, peak biomass yield, and thermal shading performance for a standalone LSC, a standalone photobioreactor, and the hybrid facade at the summer solstice in Rome.

Table 1. Sub-system efficiency and peak operational parameters, summer solstice, Rome

Parameter	Standalone LSC	Standalone PBR	Hybrid facade
Electrical efficiency (%)	4.2	0.0	4.0
PAR transmission (%)	78.0	–	71.5
Peak biomass yield (g/m^2/day)	0.0	22.5	28.4
Thermal shading coefficient	0.85	0.40	0.32

Placing the LSC in front of the photobioreactor increases peak biomass yield by 26.2% relative to the standalone photobioreactor, consistent with the mitigation of photo-inhibitory stress at the highest summer irradiance levels. The hybrid facade sacrifices only 0.2 percentage points of electrical efficiency and 6.5 percentage points of PAR transmission relative to the standalone LSC, while nearly halving the thermal shading coefficient relative to the standalone photobioreactor, indicating substantially improved solar heat gain control.

4.2. Annual Energy and Carbon Balance

Figure 1 and Table 2 summarize the annual net energy and carbon balance of the hybrid facade for the two tested climates.

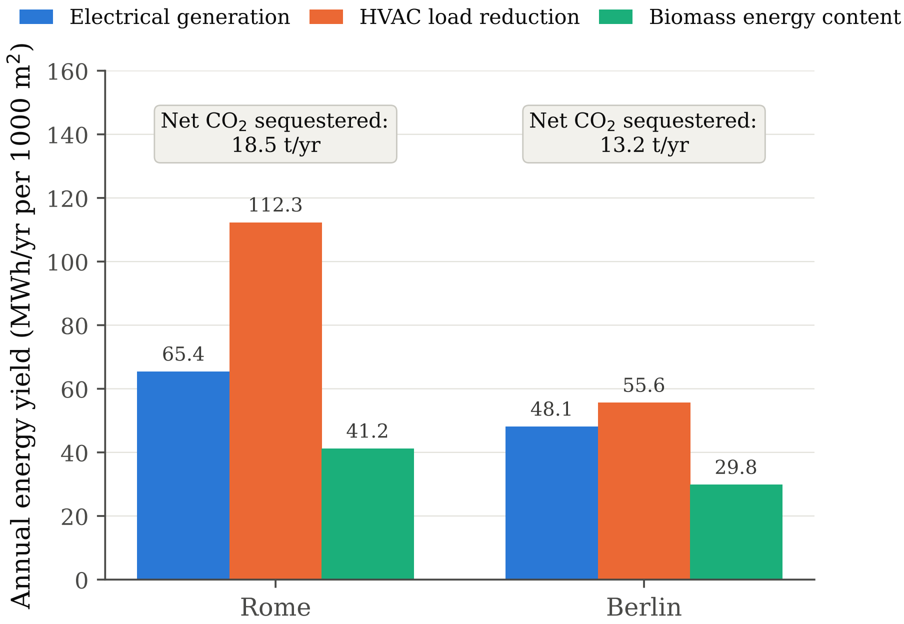

Figure 1. Annual electrical generation, HVAC load reduction, and biomass energy content of the hybrid facade per 1000 m^2, for the Mediterranean (Rome) and continental (Berlin) climate cases, with corresponding net CO_2 sequestration.

Table 2. Annual net energy and carbon balance, per 1000 m^2 facade

Climate zone	Elect. (MWh/yr)	HVAC savings (MWh/yr)	Biomass (MWh/yr)	Net CO_2 (t/yr)
Rome	65.4	112.3	41.2	18.5
Berlin	48.1	55.6	29.8	13.2

The hybrid facade sequesters 18.5 tons of CO_2 per year in Rome and 13.2 tons per year in Berlin per 1000 m^2 of installed area, turning the building envelope into an active carbon sink rather than a passive energy consumer. HVAC load reduction is the dominant energy benefit in both climates, and is proportionally larger in Rome, where higher solar loads make the improved thermal shading coefficient of the hybrid facade especially valuable. These results are broadly consistent with recent life-cycle assessments of bio-based and biologically active facade components, which likewise identify embodied and operational carbon reductions as the primary value of integrating living systems into the building envelope [13, 14].

4.3. Seasonal Variation and Long-Term Fluorophore Durability

The results in Sections 4.1 and 4.2 characterize peak summer conditions and annual totals, but the practical value of the hybrid facade also depends on how consistently it performs across the seasonal cycle and how its optical benefit degrades over the facade's service life. Table 3 reports the same sub-system metrics as Table 1, evaluated instead at the winter solstice in Rome, when both irradiance intensity and ambient temperature are substantially lower.

At the winter solstice, the biomass-yield advantage of the hybrid facade narrows to 5.4%, compared with 26.2% in summer, because photo-inhibition is no longer the binding constraint on algal growth once incident PAR falls below the saturation intensity K_S in the Haldane kinetics of Section 2.2. Under these conditions the LSC's PAR attenuation, which is fixed at 71.5% transmission regardless of season, becomes a mild yield penalty rather than a protective filter, since the standalone photobioreactor is no longer light-saturated enough to suffer inhibition. This seasonal asymmetry indicates that the hybrid facade's principal biological benefit accrues disproportionately during the highest-irradiance months, precisely when unmitigated photo-inhibition would otherwise cause the largest yield losses, and that a facade controller capable of seasonally adjusting fluorophore transmission, for example through an electrochromic or mechanically adjustable outer layer, could recover some of the winter yield penalty without sacrificing summer protection.

Table 3. Sub-system efficiency and peak operational parameters, winter solstice, Rome

Parameter	Standalone LSC	Standalone PBR	Hybrid facade
Electrical efficiency (%)	4.0	0.0	3.9
PAR transmission (%)	78.0	–	71.5
Peak biomass yield (g/m^2/day)	0.0	14.8	15.6
Thermal shading coefficient	0.85	0.40	0.34

A second consideration is the long-term stability of the LSC fluorophores themselves, since organic and perovskite-based luminescent species are known to photobleach and lose quantum yield under sustained UV exposure [8, 9]. We modeled fluorophore degradation as a first-order decay of the absorption coefficient $A_{LSC}(\lambda)$ with an empirical half-life of 8 years, drawn from accelerated-aging extrapolations reported for perovskite-derivative LSC glazing [8], and propagated this decay through the annual energy and carbon balance of Section 4.2. Over a 15-year facade service life, the resulting electrical efficiency declines from 4.2% to approximately 3.1%, a 26% relative loss, while the PAR-protective function of the LSC degrades in tandem, gradually eroding the biomass-yield advantage documented in Table 1. This suggests that the economic case for the hybrid facade depends materially on fluorophore encapsulation quality and that a mid-life glazing replacement, timed to coincide with routine facade maintenance, would be necessary to sustain the reported performance over a multi-decade building lifetime.

5. CONCLUSION

This study demonstrates the synergistic potential of coupling an optical nanotechnology, the luminescent solar concentrator, with a biological system, the microalgae photobioreactor, within a single building envelope. By managing the solar spectrum so that ultraviolet and near-infrared photons are converted to electricity while photosynthetically active radiation is preserved for biomass growth, the hybrid facade achieves simultaneous electricity generation, substantial HVAC load reduction, and measurable carbon sequestration. Future work will validate the coupled model against outdoor prototype measurements and extend the framework to multi-story facade arrays and alternative microalgae strains.

REFERENCES

[1] C. Maduta, D. D'Agostino, S. Tsemekidi-Tzeiranaki, and L. Castellazzi, "From nearly zero-energy buildings (NZEBs) to zero-emission buildings (ZEBs): Current status and future perspectives," *Energy and Buildings*, vol. 328, art. 115133, 2025.

[2] N. N. Myint, M. Shafique, X. Zhou, and Z. Zheng, "Net zero carbon buildings: A review on recent advances, knowledge gaps and research directions," *Case Studies in Construction Materials*, vol. 22, art. e04200, 2025.

[3] M. A. L. Frandoloso, S. Matana Júnior, R. C. Fritsch, A. Rempel, L. M. Colla, E. G. da Cunha, J. M. Nicolodi, J. G. Cendron, and F. L. Pinto, "The use of photobioreactors in façades for decarbonization process," *Discover Sustainability*, vol. 5, art. 327, 2024.

[4] Y. Yaman, A. Tokuç, İ. Deniz, M. A. Ezan, G. Köktürk, M. Conk Dalay, and Z. Demirel, "Photobioreactor facade panels: enhancing comfort, reducing energy use, and capturing carbon in temperate continental climates," *Systems Microbiology and Biomanufacturing*, vol. 5, no. 1, pp. 357–370, 2024.

[5] Z. Tekin, M. Al-Hammadi, G. Çalişkan, D. Irkdaş Doğu, O. Mengi, D. Deniz, and M. Güngörmüşler, "Evaluation of photobioreactor designs for potential application as microalgal façade systems," *Scientific Reports*, vol. 16, art. 11871, 2026.

[6] M. Talaei and H. Sangin, "Thermal comfort, daylight, and energy performance of envelope-integrated algae-based bioshading and static shading systems through multi-objective optimization," *Journal of Building Engineering*, vol. 90, art. 109435, 2024.

[7] J. Choi and S.-J. Kim, "A highly transparent and efficient luminescent solar concentrator based on nanosized molybdenum clusters and quantum-cutting perovskite nanocrystals," *Journal of Materials Chemistry C*, vol. 12, pp. 12026–12036, 2024.

[8] H. Yang, H. Lu, X. Wang, W. Sun, Y. Yang, W. Xiong, G. Long, J. Xu, X. Zhang, M. Yuan, and X. Li, "Recyclable luminescent solar concentrator from lead-free perovskite derivative," *Light: Science & Applications*, vol. 14, art. 297, 2025.

[9] R. A. S. Ferreira, S. F. H. Correia, L. Fu, P. Georgieva, M. Antunes, and P. S. André, “Predicting the efficiency of luminescent solar concentrators for solar energy harvesting using machine learning,” *Scientific Reports*, vol. 14, art. 4160, 2024.

[10] N. Ghaeili Ardabili, M. Elmi, and J. Wang, “Building-integrated solar delivery strategies for algae photobioreactors in cold climates,” *Buildings*, vol. 16, no. 2, art. 391, 2026.

[11] M. Dębowski, J. Kazimierowicz, and M. Zieliński, “Multi-sensing monitoring of the microalgae biomass cultivation systems for biofuels and added value products synthesis: challenges and opportunities,” *Applied Sciences*, vol. 15, no. 13, art. 7324, 2025.

[12] L. Nedaei and H. Shokrkar, “Influence of process factors and photobioreactor design on microalgae cultivation,” *Biofuels, Bioproducts and Biorefining*, vol. 2025, no. 6, pp. 2433–2456, 2025.

[13] L. Morganti, L. Vandi, J. Astudillo Larraz, J. García-Jaca, A. Navarro Muedra, and A. Pracucci, “A1–A5 embodied carbon assessment to evaluate bio-based components in façade system modules,” *Sustainability*, vol. 16, no. 3, art. 1190, 2024.

[14] R. Jakubovskis, “Biophilic façades: the potentiality of bioreceptive concrete,” *Buildings*, vol. 15, no. 20, art. 3646, 2025.

[15] K. H. Kim, M. W. Parrow, and P. Kheirkhah Sangdeh, “Microalgae-integrated building enclosures: a nature-based solution for carbon sequestration,” *Frontiers in Built Environment*, vol. 11, 2025.

[16] M. Gabr, H. Bakouch, and H. El-Taweel, “A first-order autoregressive process with weighted Lindley innovations and its applications to energy and financial data,” *Annals of Mathematics and Computer Science*, vol. 29, pp. 1–19, 2025, doi: 10.56947/amcs.v29.573.

[17] R. Obogi and M. N. Evans, “Spectral gaps and approximate invariance in Hilbert spaces,” *Annals of Mathematics and Computer Science*, vol. 30, pp. 85–92, 2025, doi: 10.56947/amcs.v30.650.

[18] T. M. Kabore and O. J.-E. Ouedraogo, “Forecasting overdispersed count time series with the DLD-INAR(1) model,” *Annals of Mathematics and Computer Science*, vol. 30, pp. 68–84, 2025, doi: 10.56947/amcs.v30.632.

[19] Z. Souleymane, B. Lamien, M. Beidari, and T. Inoussa, “Numerical simulation of pollutants transport in groundwater using deep neural networks informed by physics,” *Gulf Journal of Mathematics*, vol. 16, no. 2, pp. 337–352, 2024, doi: 10.56947/gjom.v16i2.1863.

[20] A. Hadjou Belaid, “Modelling environmental stochasticity in a stage-structured population applying stochastic differential equations,” *Gulf Journal of Mathematics*, vol. 18, no. 1, pp. 218–234, 2024, doi: 10.56947/gjom.v18i1.2402.

[21] A. Bouaicha, M. Lamnii, and S. Ngadi, “FRACCN: Fractional spline neural networks,” *Gulf Journal of Mathematics*, vol. 22, no. 2, 2026, doi: 10.56947/gjom.v22i2.4041.

[22] F. Kamalov, H. Sulieman, S. Moussa, J. Avante Reyes, and M. Safaraliev, “Powering electricity forecasting with transfer learning,” *Energies*, vol. 17, no. 3, art. 626, 2024.

[23] F. Kamalov, I. Zicmane, M. Safaraliev, L. Smail, M. Senyuk, and P. Matrenin, “Attention-based load forecasting with bidirectional finetuning,” *Energies*, vol. 17, no. 18, art. 4699, 2024.

[24] F. Kamalov, K. Rajab, A. K. Cherukuri, A. Elnagar, and M. Safaraliev, “Deep learning for Covid-19 forecasting: State-of-the-art review,” *Neurocomputing*, vol. 511, pp. 142–154, 2022.